Journal of Zhejiang University-SCIENCE C (Computers & Electronics)
ISSN 1869-1951 (Print); ISSN 1869-196X (Online)
www.zju.edu.cn/jzus; www.springerlink.com
E-mail: jzus@zju.edu.cn

Real-time motion deblurring algorithm with robust noise suppression*

Hua-jun FENG†, Yong-pan WANG, Zhi-hai XU, Qi LI, Hua LEI, Ju-feng ZHAO

(*State Key Lab of Modern Optical Instrumentation, Zhejiang University, Hangzhou 310027, China*)

†E-mail: fenghj@zju.edu.cn

Received Apr. 11, 2009; Revision accepted Sept. 29, 2009; Crosschecked Mar. 29, 2010

Abstract: In an image restoration process, to obtain good results is challenging because of the unavoidable existence of noise even if the blurring information is already known. To suppress the deterioration caused by noise during the image deblurring process, we propose a new deblurring method with a known kernel. First, the noise in the measurement process is assumed to meet the Gaussian distribution to fit the natural noise distribution. Second, the first and second orders of derivatives are supposed to satisfy the independent Gaussian distribution to control the non-uniform noise. Experimental results show that our method is obviously superior to the Wiener filter, regularized filter, and Richardson-Lucy (RL) algorithm. Moreover, owing to processing in the frequency domain, it runs faster than the other algorithms, in particular about six times faster than the RL algorithm.

Key words: Motion blurring, Motion kernel, Gaussian distribution
doi:10.1631/jzus.C0910201 **Document code:** A **CLC number:** TP317.4

1 Introduction

Blurring is common in many situations, such as capturing pictures in a plane or aircraft and shooting objects that are moving much faster than the exposure speed. To avoid this phenomenon, various stabilization work (Portilla *et al.*, 2003; Shi *et al.*, 2008; Zheng *et al.*, 2008) has been undertaken. This paper implements a motion deblurring method after the image is captured and the motion information is obtained during some other work (Chen *et al.*, 2007; Fu *et al.*, 2009). Many easy and effective methods have been developed for this purpose, such as the Wiener filter (Gonzalez and Woods, 1992), the regularized filter (Jain, 1989), and the Richardson-Lucy (RL) deconvolution algorithm (Richardson, 1972; Lucy, 1974).

The Wiener filter is based on minimizing the statistical error function, and the regularized filter is based on minimizing the criterion filter of the image to smooth the image. These two filters are effective only when the noise information is known; otherwise, it may have poor results. When the blurred image is less noisy, the result of the RL algorithm is better compared with these two methods because the Wiener filter and the regularized filter have few priors. The RL algorithm is the most common non-blind image deconvolution technique, which is an iterative restoration algorithm that maximizes a Poisson statistics image likelihood function to achieve a maximum likelihood solution when the iteration is over. The RL algorithm has two drawbacks. One is that the noise will be amplified with the increase of the number of iterations. The other is that the number of iterations cannot be ascertained, and the computing time will increase with the number of iterations.

This paper proposes a new image deblurring algorithm with a known kernel, which could produce high-quality results even if the noise information is unknown. At the same time, we could change the smoothness of the deblurring image by adjusting the parameters. This approach is much faster than the RL

* Project supported by the National Natural Science Foundation of China (No. 60977010), the National Basic Research Program (973) of China (No. 2009CB724006), and the National High-Tech Research and Development (863) Program of China (No. 2006AA12Z107)

algorithm owing to processing in the frequency domain and it can produce deblurring in real time.

2 Image motion deblurring model

First of all, the image deblurring model should be analyzed in image restoration. For motion blurring, the model could be described by a linear system (Fig. 1).

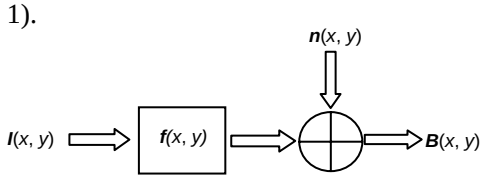

Fig. 1 Image blurring model
I: latent image; ***f***: motion kernel; ***n***: additive noise; ***B***: blurred image

Since the system is linear, the relation between the blurred image and the latent image can be expressed as

$$\boldsymbol{B}(x,y)=\boldsymbol{f}(x,y)*\boldsymbol{I}(x,y)+\boldsymbol{n}(x,y), \tag{1}$$

where * is the convolution operator, $\boldsymbol{I}(x, y)$ is the clear latent image, $\boldsymbol{f}(x, y)$ is the motion kernel, $\boldsymbol{n}(x, y)$ is the additive noise, and $\boldsymbol{B}(x, y)$ is the blurred image. In this model, the blurred image is generated from the clear image by convoluting a motion kernel and adding a noise.

As the convolution operator is linear, Eq. (1) can be changed into $\boldsymbol{B}=\boldsymbol{C}_{\boldsymbol{f}}\circ\boldsymbol{I}+\boldsymbol{n}$, where $\boldsymbol{C}_{\boldsymbol{f}}$ is the cycle matrix of $\boldsymbol{f}$, and ◦ is the multiplication operator. It can also be expressed in the frequency domain:

$$\boldsymbol{B}(u,v)=\boldsymbol{F}(u,v)\boldsymbol{I}(u,v)+\boldsymbol{N}(u,v). \tag{2}$$

The main work of image restoration is to find a clear image $\boldsymbol{I}'(x, y)$ that is the best estimation of the latent image $\boldsymbol{I}(x, y)$. In the next section, an image deblurring procedure was designed according to the model in Fig. 1 using some prior solutions.

3 Image restoration model

There are two unknown parameters in Eq. (1) in the case where the kernel is known. The first is the clear image $\boldsymbol{I}(x, y)$ which we need to identify, and the other is the noise $\boldsymbol{n}(x, y)$ added during the capturing process. Therefore it is an ill-posed problem and we can obtain only the optimal solution, not the unique one.

3.1 Definition of the probability terms

We treat the non-blind image restoration problem as a probability model to add the priors to the deconvolution process. Thus, we obtain a maximum a posterior (MAP) solution, using Bayes' theorem:

$$\boldsymbol{I}(x,y)=\arg\max_x P(\boldsymbol{I}/\boldsymbol{B})\propto P(\boldsymbol{B}/\boldsymbol{I})P(\boldsymbol{I}). \tag{3}$$

The likelihood $P(\boldsymbol{B}/\boldsymbol{I})$ of an observed image is given by the latent image and blurred image based on the convolution model $\boldsymbol{n}=\boldsymbol{B}-\boldsymbol{f}*\boldsymbol{I}$. We assume that the image noise $\boldsymbol{n}$ is modeled as a set of independent and identical Gaussian distributions (Levin *et al*., 2007). The algorithm based on this assumption is robust, and the result from the noise free image is also very good because the assumption is universally applicable. The probability $P(\boldsymbol{I}/\boldsymbol{B})$ is defined as

$$P(\boldsymbol{I}/\boldsymbol{B})\propto\exp\left(-\frac{\|\boldsymbol{B}-\boldsymbol{f}*\boldsymbol{I}\|_2^2}{2\alpha^2}\right). \tag{4}$$

The effect of the actual noise should be local when the noise satisfies distributions other than the Gaussian, especially the salt and pepper noise. To make the deblurred image smooth and fit for human vision, we assume that the first (Fergus *et al*., 2006) and second orders of derivatives obey independent Gaussian distributions. The probability $P(\boldsymbol{I})$ is defined as

$$\begin{aligned}P(\boldsymbol{I})\propto\exp(\beta(&\|d_x*\boldsymbol{I}\|_2^2+\|d_y*\boldsymbol{I}\|_2^2+\|d_{xx}*\boldsymbol{I}\|_2^2\\&+\|d_{xy}*\boldsymbol{I}\|_2^2+\|d_{yy}*\boldsymbol{I}\|_2^2.\end{aligned} \tag{5}$$

To simplify the MAP problem, we minimize an energy object function by taking the logarithm of the probability:

$$\begin{aligned}E&=E_{\mathrm{gn}}+E_{\mathrm{gd}}\\&=\|\boldsymbol{B}-\boldsymbol{c}_{\boldsymbol{f}}\boldsymbol{I}\|_2^2+w(\|\boldsymbol{c}_{d_x}\boldsymbol{I}\|_2^2+\|\boldsymbol{c}_{d_y}\boldsymbol{I}\|_2^2+\|\boldsymbol{c}_{d_{xx}}\boldsymbol{I}\|_2^2\\&\quad+\|\boldsymbol{c}_{d_{xy}}\boldsymbol{I}\|_2^2+\|\boldsymbol{c}_{d_{yy}}\boldsymbol{I}\|_2^2),\end{aligned} \tag{6}$$

where $\boldsymbol{c}_{d_x}$, $\boldsymbol{c}_{d_y}$, $\boldsymbol{c}_{d_{xx}}$, $\boldsymbol{c}_{d_{xy}}$, and $\boldsymbol{c}_{d_{yy}}$ are the cycle matrices of the gradient operator in *x*, *y* directions and each direction of the second order derivative, respectively. $\|\cdot\|_2$ is the second order norm, and $\omega=-\alpha^2\beta$ is the regularization weight of the Gaussian distribution of the image gradient.

3.2 Deconvolution

We run the derivation of Eq. (6) to minimize the energy. The problem changes into a standard minimization problem $\boldsymbol{Ax}=\boldsymbol{b}$, where

$$\boldsymbol{A}=\boldsymbol{c}_f^{\mathrm{T}}\boldsymbol{c}_f+w(\boldsymbol{c}_{d_x}^{\mathrm{T}}\boldsymbol{c}_{d_x}+\boldsymbol{c}_{d_y}^{\mathrm{T}}\boldsymbol{c}_{d_y}+\boldsymbol{c}_{d_{xx}}^{\mathrm{T}}\boldsymbol{c}_{d_{xx}}+\boldsymbol{c}_{d_{xy}}^{\mathrm{T}}\boldsymbol{c}_{d_{xy}}+\boldsymbol{c}_{d_{yy}}^{\mathrm{T}}\boldsymbol{c}_{d_{yy}}),$$
$$\boldsymbol{b}=\boldsymbol{c}_f^{\mathrm{T}}\boldsymbol{B}.$$

To solve the problem we can choose the common iterative algorithm, such as the conjugate gradient method. Since all the terms in *E* are quadratic forms, we can change Eq. (6) to the corresponding frequency domain by applying Plancherel's theorem:

$$\begin{aligned}E&=E_{\mathrm{gn}}+E_{\mathrm{gd}}\\&=\|F(\boldsymbol{B})-F(f)\circ F(\boldsymbol{I})\|_2^2+\omega\big(\|F(d_x)\circ F(\boldsymbol{I})\|_2^2\\&\quad+\|F(d_y)\circ F(\boldsymbol{I})\|_2^2+\|F(d_{xx})\circ F(\boldsymbol{I})\|_2^2\\&\quad+\|F(d_{xy})\circ F(\boldsymbol{I})\|_2^2+\|F(d_{yy})\circ F(\boldsymbol{I})\|_2^2\big).\end{aligned}\tag{7}$$

Set $\dfrac{\partial E}{\partial F(\boldsymbol{I})}=0$, and then the image estimation in the frequency domain is obtained:

$$F(\boldsymbol{I})=\frac{F(\boldsymbol{B})\circ F(\boldsymbol{f})}{|F(\boldsymbol{f})|^2+w\sum_i|F(d_i)|^2},\tag{8}$$

where $i=x, y, xx, xy, yy$. Finally the optimal solution can be obtained by applying the inverse Fourier transform: $\boldsymbol{I}^*=F^{-1}(F(\boldsymbol{I}))$.

4 Experimental results

4.1 Results of the noise-free image

We implemented our algorithm in MATLAB environment, and compared the results with some existing mature algorithms such as the regularized filter, the Wiener filter, and the RL algorithm.

Applying deconvolution in the frequency domain usually results in artifacts at the image border. We applied the Hamming window to make the gray values near the border gradually reduce to zero before image restoration, and then we obtained a good result in suppressing the border ringing. This could be implemented by a function 'edgetaper' (Gonzalez *et al*., 2004) in MATLAB.

The results of the noise-free images deblurred using the Wiener filter, regularized filter, RL algorithm, and our algorithm are shown in Fig. 2. The blurred image named 'old man' (Fig. 2a) is 532×800×3 in size, and the known kernel (Fig. 2b) is 19×27 in size. Figs. 2c–2f show the results of the regularized filter, the Wiener filter, the RL algorithm with 20 iterations, and our algorithm. Compared with the other algorithms, the resulting image of our algorithm was smoother and had fewer ringing artifacts.

The results were evaluated using the gray mean gradient (GMG) and the Laplacian operator (LS), defined as

$$\mathrm{GMG}=\frac{1}{(M-1)(N-1)}\cdot\sum_{i=1}^{M-1}\sum_{j=1}^{N-1}\sqrt{\frac{1}{2}\big(g(i+1,j)-g(i,j)\big)^2+\big(g(i,j+1)-g(i,j)\big)^2},$$

$$\begin{aligned}\mathrm{LS}=&\frac{1}{(M-2)(N-2)}\cdot\sum_{i=2}^{M-1}\sum_{j=2}^{N-1}\big|8g(i,j)-g(i-1,j-1)-g(i-1,j)-g(i-1,j+1)\\&-g(i,j-1)-g(i,j+1)-g(i+1,j-1)\\&-g(i+1,j)-g(i+1,j+1)\big|,\end{aligned}$$

where the size of $g(m, n)$ is $M\times N$. Smaller values of GMG and LS indicate fewer ringing artifacts and smoother images, and thus higher quality. The smallest GMG and LS (Table 1) indicated that our algorithm is the best among these algorithms.

Table 1 Objective evaluation of the algorithms

Method	GMG	LS	*T* (s)
Regularized filter	4.4730E-5	0.0984	3.9112
Wiener filter	4.5663E-5	0.1012	2.9438
RL algorithm	4.0974E-5	0.0819	25.3428
Our algorithm	3.5409E-5	0.0671	2.8333

GMG: gray mean gradient; LS: Laplacian operator; *T*: running time

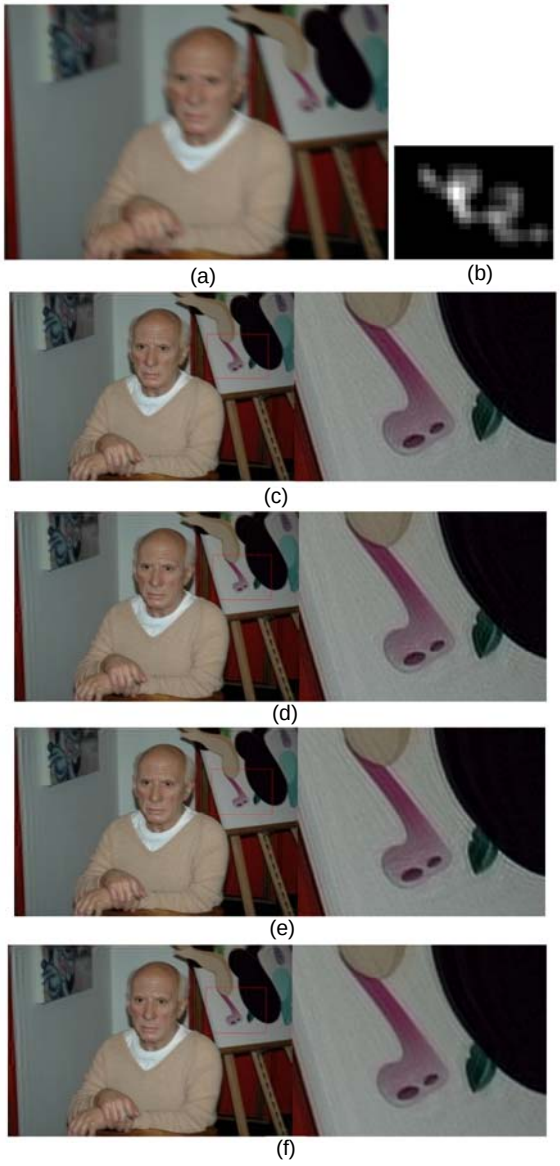

Fig. 2 The blurred, deblurred, and local enlarged images
(a) Blurred image (532×800×3); (b) Kernel (19×27); (c) Regularized filter result; (d) Wiener filter result; (e) RL result; (f) Our result

Time complexity is also one of the common metrics to evaluate the quality of an algorithm. Our method is very fast because of processing in the frequency domain, and the running time was less than 3 s (the actual time depends on the image size).

In short, our method is better for quality and running time for the noise-free image than the three general algorithms.

4.2 Results of various noised images

To test the noise robustness of our method, the process shown in Fig. 3 was applied. First, the clear image was blurred with the motion kernel and then degraded by various noises. After that, we deblurred the degraded images using the Wiener filter, the regularized filter, the RL algorithm, and our algorithm, respectively. The deblurred images are given in Fig. 4, and the values used to evaluate the results given in Table 2, showing that our method is better than the other three algorithms.

The images used in the deblurring process are shown in Fig. 4. The blurred image named 'flying-plane' whose size is 299×450×3 and the known kernel whose size is 6×12 are shown in Fig. 4a. Our results (Fig. 4f) were better than the results of the regularized filter (Fig. 4c), the Wiener filter (Fig. 4d), the RL algorithm (Fig. 4e) for all the four noises.

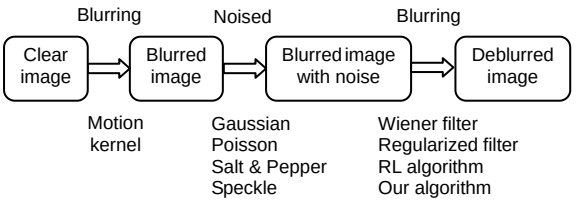

Fig. 3 Deblurring model for noised images

Table 2 Objective evaluation of the algorithms based on various noises

Method	Gaussian noise*			Poisson noise		
	GMG	LS	*T* (s)	GMG	LS	*T* (s)
Regularized filter	9.0311E-4	1.6433	1.4957	1.4573E-4	0.1199	1.4613
Wiener filter	0.0013	2.2694	1.1270	1.5617E-4	0.1342	1.1365
RL algorithm	8.9187E-4	1.5787	8.3091	1.3304E-4	0.1002	8.2236
Our algorithm	1.1446E-4	0.1687	1.0002	1.1007E-4	0.0737	0.9997
Method	Salt & pepper noise**			Multiplicative noise***		
	GMG	LS	*T* (s)	GMG	LS	*T* (s)
Regularized filter	0.0021	3.5809	1.5105	0.0013	2.4144	1.5291
Wiener filter	0.0030	4.9783	1.1271	0.0020	3.3417	1.0972
RL algorithm	0.0016	2.7133	8.3932	0.0013	2.2373	8.3952
Our algorithm	2.1830E-4	0.3364	1.0057	1.5257E-4	0.2390	1.0058

With a variance of *0.001, **0.02, ***0.01, respectively. GMG: gray mean gradient; LS: Laplacian operator; *T*: running time

Fig. 4 The blurred, noised, and deblurred images

(a) Blurred image (299×450×3) and kernel (6×12); (b) Noised images; (c) Regularized filter results; (d) Wiener filter results; (e) RL results; (f) Our results. In (b)–(f), the subfigures from left to right are results of Gaussian noised (with a variance of 0.001), Poisson noised (standard), salt & pepper noised (with a density of 0.02), and multiplicatively noised (with a variance of 0.01) images, respectively

In addition, the GMG, LS, and time complexity were used to evaluate the results of the noised blurred image. In terms of performance in suppressing the general noise, our results were better than the others. Meanwhile, the running time was shorter than the others and in particular our algorithm was seven times faster than the RL algorithm.

5 Conclusion

We have proposed a probability model based on the priors to deblur a motion blurred image. The model includes the Gaussian distribution noise to fit the natural noise distribution and the first and second orders of derivatives to satisfy Gaussian distribution to

suppress the non-uniform noise. It outperforms the previous approaches such as the Wiener filter, the regularized filter, and the RL algorithm. Processing in the frequency domain reduces the time taken, and our approach is much faster than the RL algorithm. In conclusion, we propose an algorithm with high-quality results, high de-noising capacity, and fast speed. This algorithm could be applied to real-time image restoration with noise robustness.

References

Chen, X.C., Cao, F.M., Jin, W.Q., 2007. Recursive model of forward motion blurred image based on polar coordinates. *Acta Photon. Sin.*, **36**(3):552-556.

Fergus, R., Singh, B., Hertzmann, A., Roweis, S.T., Freeman, W.T., 2006. Removing camera shake from a single photograph. *ACM Trans. Graph.*, **25**(3):787-794. [doi:10.1145/1141911.1141956]

Fu, Z.L., Feng, H.J., Xu, Z.H., Li, Q., Mao, C.J., 2009. Restoration of the image blurred by motion based on high-speed CCD motion detection. *Opto-Electron. Eng.*, **36**(3):69-73.

Gonzalez, R.C., Woods, R.E., 1992. Digital Image Processing. Addison-Wesley, New York, NY.

Gonzalez, R.C., Woods, R.E., Eddins, S.L., 2004. Digital Image Processing Using MATLAB. Pearson Prentice Hall, Upper Saddle River, NJ, USA.

Jain, A.K., 1989. Fundamentals of Digital Image. Prentice-Hall, Inc., Upper Saddle River, NJ, USA.

Levin, A., Fergus, R., Durand, F., Freeman, W.T., 2007. Image and depth from a conventional camera with a coded aperture. *ACM Tran. Graph.*, **26**(3), Article 70. [doi:10.1145/1276377.1276464]

Lucy, L., 1974. An iterative technique for technique for the rectification of observed distributions. *Astron. J.*, **79**(6):745-754. [doi:10.1086/111605]

Portilla, J., Strela, V., Wainwright, M.J., Simoncelli, E.P., 2003. Image denoising using scale mixtures of Gaussians in the wavelet domain. *IEEE Trans. Image Process.*, **12**(11):1338-1351. [doi:10.1109/TIP.2003.818640]

Richardson, W.H., 1972. Bayesian-based iterative method of image restoration. *J. Opt. Soc. Am.*, **62**(1):55-58. [doi:10.1364/JOSA.62.000055]

Shi, L., Su, X.Q., Xiang, J.B., 2008. An electronic image stabilization method based on feature block matching. *Photon J.*, **37**(1):202-205.

Zheng, X.F., Chen, Y.T., Xu, Z.H., 2008. A fast electronic image stabilization algorithm for tranlational and rotational motion compensation. *Acta Photon. Sin.*, **37**(9):1890-1894.